Imaging of alkyne-functionalized ruthenium complexes for photoactivated chemotherapy

Busemann, A.

1

INTRODUCTION

1.1 DNA as target of anticancer metallodrugs

In 1965, Barnett Rosenberg unexpectedly discovered the anticancer property of cis-dichlorodiammineplatinum(II), better known as cisplatin.[1] Since 1978, cisplatin is available for clinical practice and is used as chemotherapeutic agent for a wide range of tumors, and notably for metastatic testicular and ovarian cancer.[2] Cisplatin becomes cytotoxic upon hydrolysis, leading to the binding of the complex to the purine bases of DNA (N7 of guanine and adenine). This interaction results in cross-linked DNA.[3] Subsequently, repair, replication, and transcription of the nucleic acid is no longer possible, causing apoptosis of the cell. The main drawbacks of cisplatin are the inherent or acquired resistance of cells and side effects like nephrotoxicity, ototoxicity, and neurotoxicity caused by non-specific binding of the complex to other biomolecules.[2] New derivatives of the platinum drug were synthesized (carboplatin and oxaliplatin, Figure 1.1) to improve on those side effects, but these drugs require higher dosages and are effective against a smaller range of tumors.[4]

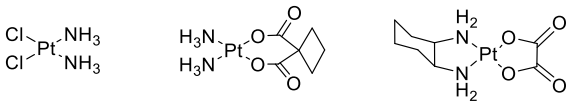

cisplatin carboplatin oxaliplatin

Figure 1.1. Chemical structures of cisplatin and its derivatives carboplatin and oxaliplatin.

Other transition metal-based anticancer compounds were investigated to find complexes with a higher selectivity towards cancer cells and to keep side effects to a minimum. Inspired by the mode of action of cisplatin, these metallodrugs were designed to interact with DNA and to induce apoptosis. Ruthenium-based anticancer agents contain chloride ligands as leaving groups for effective hydrolysis, which enables covalent binding to DNA.[5] In addition, polyaminocarboxylate, arylazopyridine, polypyridyl, or arene ligands were used to induce π-π stacking with the DNA base pairs, and to intercalate with DNA.[6]

In the complex [Ru(II)(η^6–biphenyl)(ethylenediamine)(Cl)]$^+$ (RM175) for example, the hydrophobic arene ligand is used to stabilize the oxidation state of ruthenium and to facilitate drug uptake by passive transport (Figure 1.2).[7] In addition, the biphenyl ligand can intercalate between DNA base pairs. The *in vitro* cytotoxicity of RM175 is similar to that of carboplatin (in A2780 human ovarian cancer cells: 5, 6, and 0.6 μM for RM175, carboplatin, and cisplatin, respectively),[8] and the level of DNA-Ru adduct formation is similar to DNA platination by cisplatin.[9] Studies on

single-strand DNA as well as on duplex DNA, analyzed by NMR spectroscopy, revealed an efficient binding of the ruthenium center with N7 of guanine.[9, 10] Competition reactions in the presence of proteins did not affect the binding, pointing towards DNA as primary target of RM175.[11] *In vitro* studies in wild type HCT116 colorectal cancer cells showed that the treatment of cancer cells with RM175 results in the accumulation of the suppressor proteins p53, p21, and BAX.[12] Those proteins induce cell cycle arrest (in G1 and G2 phase) and apoptosis in case of damaged DNA.

Another example is indazolium *trans*-[tetrachlorobis(1H-indazole)ruthenate(III)], better known as KP1019. Developed by Keppler and coworker (Figure 1.2),[13] KP1019 acts against colon cancer and is one of the most famous and successful examples of ruthenium-based anticancer drugs since it reached clinical trial.[13] Activation by reduction of KP1019 in cells leads to the formation of the Ru(II) species with more labile Ru-Cl bonds.[14] The drug binds in a non-covalent manner to human serum albumin (HSA),[15] and it is assumed that specific transport *via* plasma protein transferrin (Tf) leads to the accumulation of the drug in cancer cells. In the cells, KP1019 interacts with DNA *via* monofunctional N7 coordination of the purines of guanosine 5′-monophosphate (GMP) and adenosine 5′-monophosphate (AMP).[14] The drug causes DNA unwinding, resulting in weak bending. KP1019 induces apoptosis *via* the intrinsic (mitochondrial) pathway.[13] The drug finished Phase I of clinical trials successfully without severe side effects. Due to its low solubility, the clinical testing proceeded with the water-soluble sodium salt analogue NKP1339.[16]

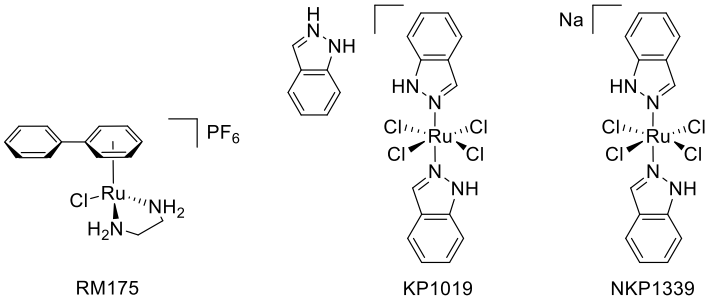

RM175 KP1019 NKP1339

Figure 1.2. Chemical structure of the anticancer compounds RM175, KP1019, and NKP1339.

1.2 Cytotoxicity beyond DNA interaction

The RAPTA family consists of ruthenium-based anticancer complexes with the monodentate ligand 1,3,5-triaza-7-phosphatricyclo[3.3.1.1]decane (pta) and η^6-arene. The two remaining coordination sites are occupied by chloride or bridging carboxylate ligands, inspired by cisplatin and its derivatives (Figure 1.3). The

complexes are air-stable and are soluble in polar organic solvents and water.[6] RAPTA-C is the prototype compound of the RAPTA family. It has a high *in vitro* EC_{50} value (507 μM for TS/A mouse adenocarcinoma), but shows selectivity for cancerous over healthy cells (EC_{50} >1000 μM for non-tumorigenic HBL-100 human mammary cell line).[6] In addition, *in vivo* studies showed the reduction of the number of lung metastases from mammary carcinoma in mice after administration of the metallodrug.[17] The interaction of RAPTA-C with 2′-deoxyguanosione 5′-monophosphate (dGMP) was investigated and compared to that of KP1019.[18] RAPTA-C hydrolyzes rapidly to form the corresponding aqua complex and therefore, the complex is more reactive towards dGMP than KP1019. However, since no direct correlation between the binding to dGMP and its cytotoxicity could be found, it was hypothesized that proteins are the major target of RAPTA-C rather than DNA. It is assumed that the bulky pta ligand causes unfavorable steric interaction with DNA, leading to a preferred protein binding.[19] This hypothesis was confirmed by studies of the ruthenium complex in the presence of critical intracellular proteins (such as ubiquitin, cytochrome c, and superoxide dismutase) in which the interaction of RAPTA-C with these proteins was shown.[20]

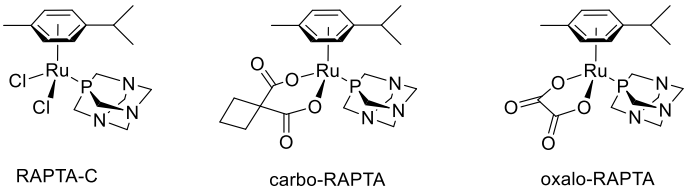

Figure 1.3. Chemical structures of anticancer drugs of the RAPTA family, derived from cisplatin and its derivatives.

Nowadays, the "DNA paradigm" that metallodrugs only cause cytotoxicity by direct damage of the DNA,[21] is not valid anymore. Even for cisplatin, protein interactions are reported in the literature *e.g.* with HSA and Tf.[22, 23] Therefore, the interaction of metallodrugs with proteins should not be neglected. Metallodrug-protein adducts can be the cause of drug cytotoxicity, side effects (*in vivo*), or be responsible for resistance mechanisms.[24] The interaction between the drug and a protein can be covalent (direct binding of an amino acid residue to the metal center) or non-covalent (*e.g. via* π-π stacking, hydrophobic, or electrostatic interactions). In addition, the drug can act as specific protein inhibitor. Typical proteins that have been shown to be inhibited by metallodrugs are kinases, estrogen receptors, cysteine-containing proteins, or glutathione S-transferase. A detailed overview can be found in reviews by Hartinger and Meggers.[25, 26]

Targeting a protein that is involved in cancer-correlated pathways increases the chances to obtain a drug which is usually more toxic for cancerous cells than for healthy cells. This selectivity is essential in anticancer therapy as it increases the effect of the drug while lowering the probability of side effects.[6] According to Bergamo, targeted metallodrugs interfere with the specific target and thus control metastasis rather than having a general/unspecific antitumor activity caused by interaction with nucleic acids, mitochondria or proteins commonly expressed and used by all kinds of cells.[27] However, Dyson points out that with this approach targeted chemotherapeutics are so specific, that only certain cancer types are treated. In contrast to targeted chemotherapy, "classical" non-targeted drugs such as cisplatin can be used widely.[6] Instead of looking for specific biological targets, selectivity can also be triggered by physical factors. KP1019 and RAPTA-C are thought to be activated by reduction.[14, 17, 28] Since cancerous cells are generally more acidic than healthy cells, reduction of *e.g.* Pt(IV) or Co(III) complexes is more efficient in cancer cells. More details about "activation by reduction" of metal complexes can be found in reviews by Lippard and Heffeter.[29, 30]

1.3 Phototherapy - selectivity based on light activation

Another type of selectivity can be acquired using photoactivation. In this physical approach, light triggers the activation of a biologically inactive but photoreactive compound, called a photoactivatable prodrug (Scheme 1.1). Upon injection, the prodrug distributes throughout the body, and later, local irradiation with visible light induces an increased biological activity of the drug at the tumor site. With this method, undesired interactions of the drug with healthy cells, in particular in non-irradiated organs, are minimized.

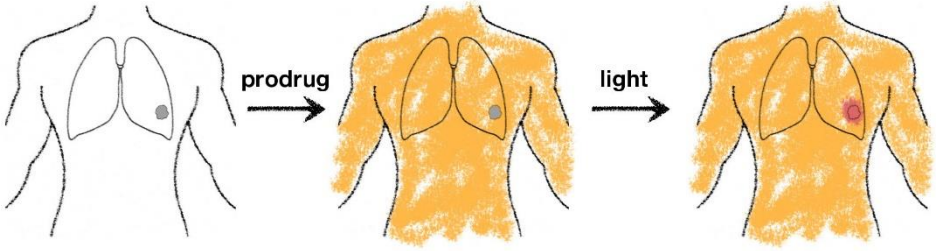

Scheme 1.1. A non-toxic prodrug (orange) is administered to the patient with a tumor (grey) and activated in a spatially and temporally controlled way by visible light. The activated drug (red) selectively acts only at the irradiated area.

There are two main types of phototherapy in cancer treatment: photodynamic therapy (PDT) and photoactivated chemotherapy (PACT). In PDT, a photosensitizer (PS) absorbs a photon and is thereby excited to a singlet state (Scheme 1.2). *Via* intersystem crossing (ISC), an excited triplet state is reached. In PDT type 2, this excited triplet state is quenched by molecular oxygen ($^3O_2$) and energy transfer leads to the formation of singlet oxygen ($^1O_2$). The highly reactive $^1O_2$ oxidizes biomolecules, which produces an excess of reactive oxygen species (ROS) that may cause cell death. In PDT type 1, the excited triplet state reacts directly with biomolecules; electron transfer produces free radicals that may also react with $^3O_2$ to produce superoxide. Here as well, increased ROS level lead to cell death. Phototoxicity in PDT may occur through three pathways: direct tumor cell killing, vascular damage (causing nutrient depletion), and/or an immune response.[31] In PDT $^1O_2$ production is a catalytic process, meaning that the PS is not consumed but it can turnover. Eosin was the first photosensitizer used in PDT to treat skin cancer.[32] Hereafter, the first porphyrin-based PDT agent, haematoporphyrin, was introduced. Its derivative, Photofrin, has become the first PDT drug approved for clinical use and is still the most widely used PS in cancer treatment.[32] Other examples of PDT agents approved by the FDA are Foscan (Figure 1.4), Levulan, Metvix, and Padeliporfin (WST11). Metal complexes can also act as PDT agents. The ruthenium-based photosensitizer TLD1433 was developed by McFarland and co-workers (Figure 1.4). TLD1433 is non-toxic in the dark, but upon red light activation it shows promising cytotoxicity against promyelocytic leukemia cells (HL-60).[33] This photosensitizer entered clinical trials for the treatment of bladder cancer and finished Phase I successfully.[34] For now, harmful side effects such as long lasting photosensitivity still affect patients receiving currently approved PDT treatment.[35] In addition, because PDT requires the presence of cellular oxygen to create ROS, it is less effective when oxygen concentration at the irradiated tumor site is low. This limits the effectiveness when treating tumors with large hypoxic regions. These tumors tend to be harder to treat with traditional chemotherapy methods, as indicated by the lower survival of patients with such tumors.[36, 37]

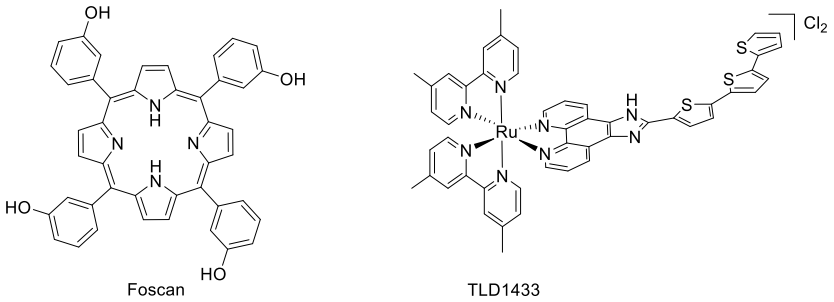

Figure 1.4. Chemical structure of the PDT photosensitizers Foscan and TLD1433.

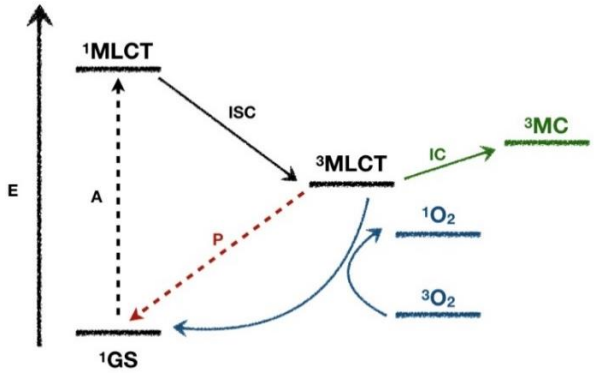

Scheme 1.2. Jablonski diagram of the photoactivation of d^6 transition metal complexes and their physical relaxation pathways in phototherapy. In the presence of molecular oxygen, photodynamic therapy (PDT) can lead to the production of reactive oxygen species (ROS) such as $^1O_2$ (in blue). In photoactivated chemotherapy (PACT), population of the ^{3}MC state leads to ligand substitution (in green). Dashed lines indicate processes involving photons. Non-radiative decay from the ^{3}MLCT and ^{3}MC state are omitted for clarity. Abbreviations: A = absorption, ISC = Intersystem crossing, IC = internal conversion, P = phosphorescence.

PACT agents, in contrast, can be utilized in low oxygen conditions, making them suitable for treating hypoxic tumors. The term PACT was introduced by Sadler and describes an inorganic photocaging strategy in oncology.[38] PACT utilizes the photochemical properties of d^6 transition metals like Rh(III), Pt(IV), Ru(II), and Co(III) to create metallodrugs that are non-toxic until light irradiation triggers activation.[38, 39] Exposure of the PACT agent to light causes an irreversible chemical change of the metal complex leading to the formation of a biologically active species (Scheme 1.3). In the case of ruthenium-based PACT agents, this activation is based on photosubstitution. Light irradiation creates a singlet metal-to-ligand charge transfer state (^{1}MLCT) and *via* ISC a triplet metal-to-ligand charge transfer state (^{3}MLCT) is reached. Due to the distorted coordination spheres of PACT agents, a low-lying triplet metal-centered state (^{3}MC) is available that can thermally be

populated from the photochemically generated ^{3}MLCT state. The ^{3}MC state has a dissociative character due to an electron being promoted in an antibonding dσ* orbital, which leads to the dissociation of a ligand and its substitution by a solvent molecule (Scheme 1.2). Quenching of the ^{3}MLCT state by the ^{3}MC state causes PACT agents to be usually non-emissive, and to show low $^1O_2$ quantum yields.[40, 41] The light-induced cytotoxicity can be caused by the interaction of cellular targets such as proteins or DNA with either the released ligand,[42-46] the metal species,[40, 47] or both. Almost any mode of action can be foreseen for a metal-based PACT compound, which opened a new field of research to identify the active species and its targets. PACT has not reached the clinics yet.

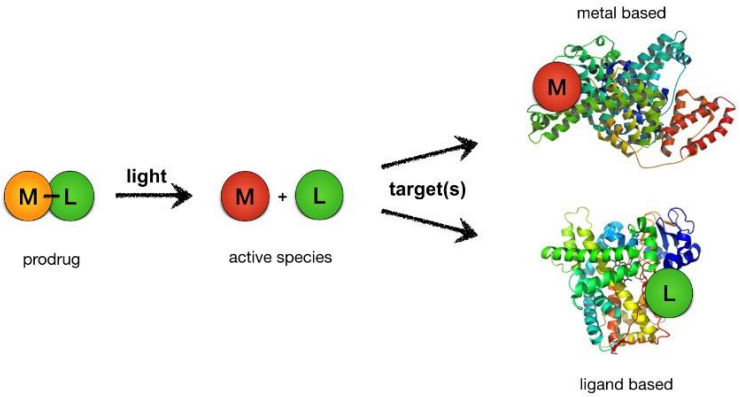

Scheme 1.3. General mechanism of PACT. A non-toxic prodrug is activated by light to generate the active species, which can be either the metal ion (M), the ligand (L), or both. The interaction with biomolecules such as proteins or DNA leads to the cytotoxicity at the irradiated tumor site.

1.4 Studying metal-protein interactions

1.4.1 Traditional methods to study interactions

In order to acquire insight on the mode of action of new metallodrugs, a variety of analytical methods has been used that allow for studying the interaction between the drugs and model proteins. The most frequently used proteins in this context are: bovine serum albumin (BSA), a model for human serum albumin (HSA), which is one of the main transport proteins in the blood; hen egg white lysozyme (HEWL), which is a histidine-rich protein and has been used a lot to model the interaction of metal compounds with this amino acid; and cytochrome c (cyt c), which is localized in the mitochondria and plays a crucial role in apoptotic pathways. Furthermore, ubiquitin (regulatory protein) and metallothionein-2 (MT-2, a cysteine-rich protein responsible for metallodrug resistance) have also been utilized. The most frequently

used experimental techniques to study metallodrug-protein interactions are introduced below.

X-ray diffraction (XRD) analysis allows for structure elucidation of metal-protein adducts. Information about possible ligand dissociation, the oxidation state of the metal center, as well as the binding sites on the biomolecule, can be obtained with atomic accuracy. For example, the XRD analysis of a KP1019-HSA adduct revealed that two ruthenium centers bind to histidine residues His146 and His242 in the hydrophobic core of albumin.[48] In addition, the crystal structure showed that all ligands dissociated from the ruthenium center before the metal ion bound covalently to HSA (Figure 1.5). The disadvantage of this method is the challenging preparation of single crystals of metal-biomolecule adducts and the non-biological conditions that are enforced during crystal growth (*e.g.* high metal complex and/or protein concentration are used, or protein crystals are soaked with the metallodrug). In addition, the structure only shows a final state, and no dynamics. The processes of ligand dissociation in solution are difficult to study.[49]

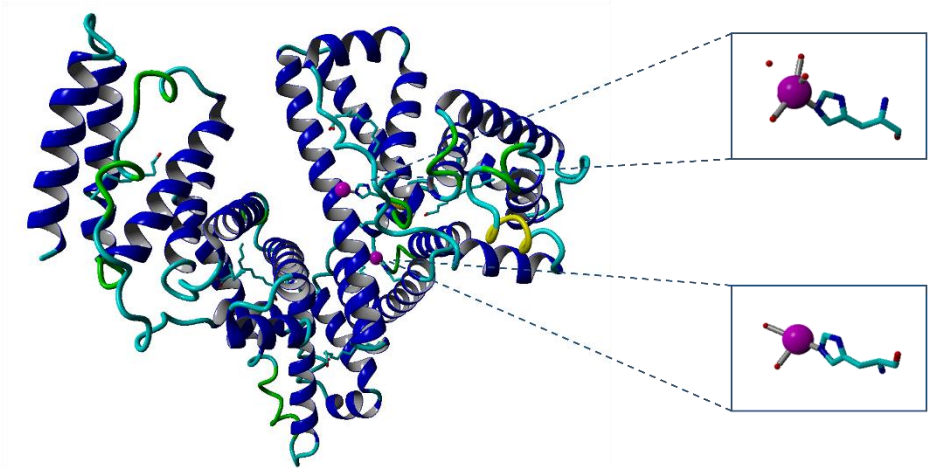

Figure 1.5. XRD structure of the KP1019-HSA adduct. All ligands are dissociated before binding of the ruthenium ion occurred at the histidine residues.[48]

Circular Dichroism (CD) spectroscopy enables the study of conformational changes in the secondary structures of DNA and proteins caused by metalation. The alteration of the absorption of circularly polarized light is a measurement of the interaction between the metal complex and the biomolecule. Often, CD measurements are performed in combination with fluorescence spectroscopy. The group of Keppler used CD to investigate the interaction of KP1019 with HSA.[50] KP1019 interactions with HSA lead to the loss of helical stability of the protein. The

relative fluorescence intensity of HSA decreased in the presence of the ruthenium complex, implying that conformational changes occurred close to the fluorescent tryptophan residue.

Electron spray ionization mass spectrometry (ESI-MS) is one of the most frequently used methods for the analysis of metal-bound proteins reported in literature. The soft ionization technique preserves most metal-protein interaction,[51] revealing the composition of the ligand-metal adducts, and enabling the quantification of metal centers bound to one protein. Casini performed ESI-MS experiments to study the interaction of RAPTA-C, carbo-RAPTA, and oxalate-RAPTA complexes with cyt c and HEWL.[52] The highest cyt c metalation was achieved with RAPTA-C, probably due to the good leaving group (chloride). A lower reactivity of the RAPTA complexes was observed for HEWL. RAPTA-C showed a preferred interaction with histidine residues at the protein surface of HEWL. The reactivity of RAPTA-C with MT-2 compared to cisplatin was also investigated by Casini.[53] The study showed that the affinity of RAPTA-C to MT-2 is lower than that of cisplatin, probably due to the presence of the arene ligand. Cysteine residues are the favorite binding site of the ruthenium center, and MT-2 can abstract RAPTA-C from competitive proteins in solution, giving insight in possible resistance mechanism and detoxifications of the drug. Glutathione (GSH, an abundant antioxidant) might also be involved in the detoxification of RAPTA-C. Their interaction was investigated by ESI-MS and the binding was confirmed.[54] In addition, GSH is able to disrupt an existing protein adduct of RAPTA-C and ubiquitin.

All these studies of metallodrug-protein adduct formations are usually performed with an isolated protein, sometimes in the presence of a few competitive targets. They provide chemical information about the reactivity of the tested metal complex. However, such controlled experiments do not resemble the complex environment of a cell since the conditions of the investigations are oversimplified and concentrations and protein-metal ratios are optimized for the analysis technique, rather than mimicking concentrations found in a cell. Therefore, techniques that identify the drug target in the cell and/or cell lysate are also necessary, in order to obtain a better insight on the mode of action of metallodrugs under physiological conditions.

1.4.2 Metalloproteomics

The observed cytotoxicity of a metal complex is often correlated to its cellular uptake. Inductively coupled plasma – mass spectrometry (ICP-MS) allows for quantitative analysis of the metal content in cell lysate after cell uptake or

fractionation experiments. The technique is element specific and allows for the analysis of *in vivo* samples as well.[51] Dyson *et al*. studied the differences in cellular uptake and subcellular distribution of NAMI-A, KP1019, and cisplatin, to be able to explain their different behavior in cisplatin-resistant and sensitive cells.[55] Ho and coworkers showed that outer membrane protein (OmpF), a cation-selective pore for small hydrophilic molecules in *E.coli*, plays a key role in the transportation of [Ru(tpy)(bpy)(Cl)]Cl (where tpy = 2,2′:6′,2″-terpyridine and bpy = 2,2′-bipyridine) into the cell.[56] The amount of ruthenium-based drug in the cell was quantified by ICP-MS measurements and a direct correlation between drug uptake and the presence of transport protein OmpF was indicated.

The combination of ICP-MS with separation techniques such as chromatographic columns (liquid chromatography, LC; high-performance liquid chromatography, HPLC; size exclusion chromatography, SEC; capillary electrophoresis, CE) enables the protein profiling of complex biological mixtures and can help to identify drug binding partners. The different types of MS hyphenation were reviewed several times.[51, 57-59] In addition, gel electrophoresis (GE) is also used for the separation of complex samples prior to MS analysis. In 2D GE, the biological sample is first separated based on isoelectric properties, followed by separation based on molecular weight. Dyson and co-workers investigated the difference in protein binding of NAMI-A and cisplatin with 2D GE and MS.[60] The quantification of the binding level of the two drugs to HSA, transferrin (Tf), and BSA were investigated, and the results demonstrated that NAMI-A is significantly less toxic than cisplatin, probably due to a different binding mode to the proteins (weaker interactions). Cheng *et al.* used 2D GE to compare the proteomic profiles of *E.coli* after treatment with different ruthenium complexes (Figure 1.6a).[61] After treatment, major effects were observed on transport proteins and oxidoreductases but also on hydrolases, stress-regulated proteins, and carbohydrate-related reactions compared to non-treated *E.coli* (Figure 1.6b and c). In addition, comparison of the different protein expressions after treatment demonstrated that an alteration of the bidentate ligand results in a change of the mode of action of the metallodrug.

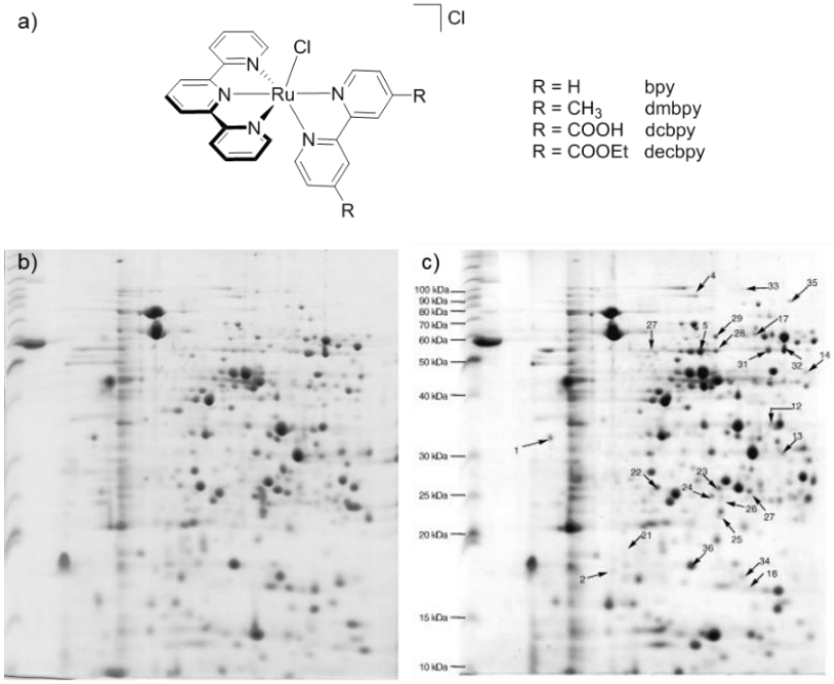

Figure 1.6. Ruthenium-based complexes with modified bpy ligands used by Cheng (a), 2D gel containing proteins of E.coli after control reaction without ruthenium complex (b), and 2D gel containing proteins of E.coli affected by ruthenium complex [Ru(tpy)(bpy)(Cl)]Cl] at 160 μM (c).[61]

Other methods used for the analysis of biological samples are multidimensional protein identification technology (MudPIT),[62, 63] functional identification of target by expression proteomics (FITExP),[64] isotope-coded affinity tag (ICAT),[65] and surface enhanced laser desorption ionization time-of-flight mass spectrometry (SELDI-TOF MS).[66] They are not discussed in further details in this introduction.

1.4.3 Drug pull-down

The techniques mentioned above provide information regarding the effect of a drug on the proteasome of a cell. To identify the actual target of a drug, its binding partners need to be isolated and analyzed. This can be achieved in a so-called pull-down assay (Scheme 1.4). Such assays are used in chemical biology for the identification of protein-protein interactions, but they can also be applied to study metal-protein interactions. In order to perform a pull-down assay, the drug (in red) is functionalized with a handle (in blue, *e.g.* a biotin, azide, or alkyne moiety). After incubation of this drug derivative with lysate or cells, a reporter tag (in green) binds to the handle. This tag allows for the separation of the metallated proteins from the

unbound proteins. Depending on the reporter tag, this separation can be achieved *e.g. via* gel electrophoresis or affinity purification. After the enrichment of the metallated proteins, the targets are analyzed by MS and identified.

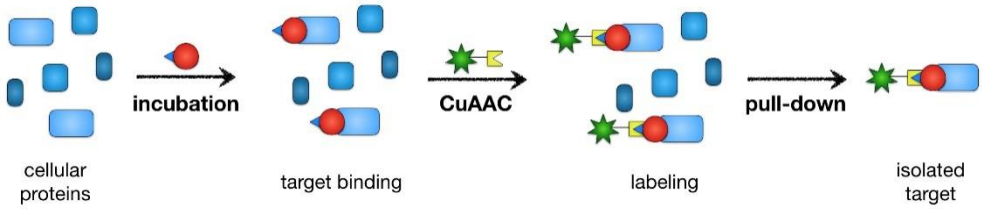

Scheme 1.4. Drug pull-down experiments allow for the identification of the drug binding partners. The drug (in red), functionalized with a handle (in blue), is incubated and labeled with a reporter tag (in green, here *via* CuAAC). This method allows for the separation of the metallated proteins. The isolated protein targets can be further analyzed and identified by MS.

In recent years, several groups performed pull-down assays to study the interaction of their metal-based drug with proteins. The first example of a drug pull-down experiment involving metallodrugs was reported by Hartinger and co-workers, investigating the targets of RAPTA-C. The complex was functionalized with a biotin handle that allowed for the immobilization of the drug *via* streptavidin-modified beads (Figure 1.7).[67] The drug derivative was exposed to human cancer cell lysates of ovarian cancer (CH1), and the metal-protein adducts were separated from unbound proteins by centrifugation. 15 cancer-related target proteins were identified with high resolution MS. The researchers were able to correlate the isolated proteins to the antimetastatic properties of the drug. A similar approach was used more recently by Meier *et al.* to profile the targets of another ruthenium(arene) complex.[68] After incubation of the biotin-functionalized derivative of the drug with the cell lysate of HCT116 colon carcinoma cells, the isolated adducts were analyzed by MS. In addition, the effect of the drug on the protein expression of HCT116 colon carcinoma cells after drug treatment was determined (response profiling) and correlated to the proteins isolated earlier *via* the pull-down assay. Bioinformatic analysis enabled the researcher to identify and also justify the structural protein plectin as possible target. The biotin handle used in these examples leads to drastic modifications of the chemical properties of the drug, which may in turn change its biological properties, such as cellular uptake and intracellular distribution. The use of such large handles is limited to fishing protein

targets in a cell lysate, while protein target identification in living systems may require the development of smaller handles.

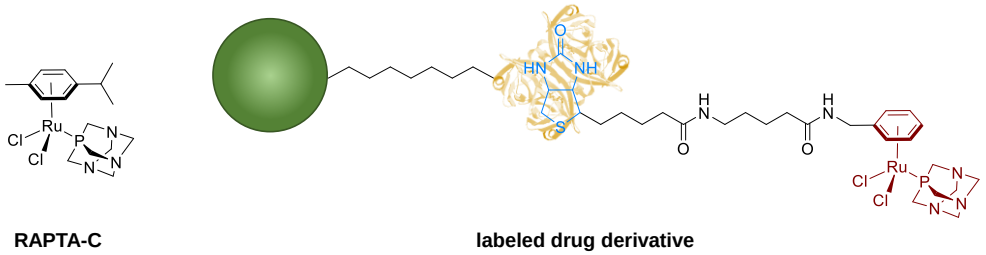

Figure 1.7. Structure of RAPTA-C and the drug derivative used in drug pull-down by the Hartinger group, bound to streptavidin-modified beads.

Indeed, if treating living cells with a handle-functionalized drug to deliver information on the mode of action of the drug without the handle, then such handle must be as small as possible, so that its presence only minimally interferes with the biological activity of the drug. Very small handles such as azide or terminal alkyne groups represent attractive alternatives. DeRose and co-workers synthesized azide-functionalized cisplatin derivatives and incubated *Saccharomyces cerevisiae* with these drug derivatives. After isolation of the DNA and RNA, fluorophore labeling *via* Cu(I)-catalyzed azide-alkyne cycloaddition (CuAAC, explained in section 1.5) in gel electrophoresis confirmed the interaction of the complexes with these biomolecules, as expected for cisplatin derivatives.[69, 70] In addition, Cunningham *et al.* investigated additional protein targets in drug-treated *S. cerevisiae*, by labeling the azide-functionalized platinum complex with biotin *via* CuAAC. This tag allowed for affinity purification and isolation of the Pt-protein adducts (Figure 1.8a).[71] They found several protein targets involved in the endoplasmic reticulum stress response. Che and co-workers also used click handles, but instead of azides, they functionalize their gold-based anticancer complexes with an alkyne click handle and a photoaffinity moiety (Figure 1.8b).[72, 73] Irradiation with UV light led to the covalent binding of the complex to the protein. Biotin labeling *via* CuAAC allowed for pull-down experiments. The studies revealed that some of their complexes interact with mitochondrial chaperons in HeLa cells,[72] while others show an affinity to several molecular targets.[73]

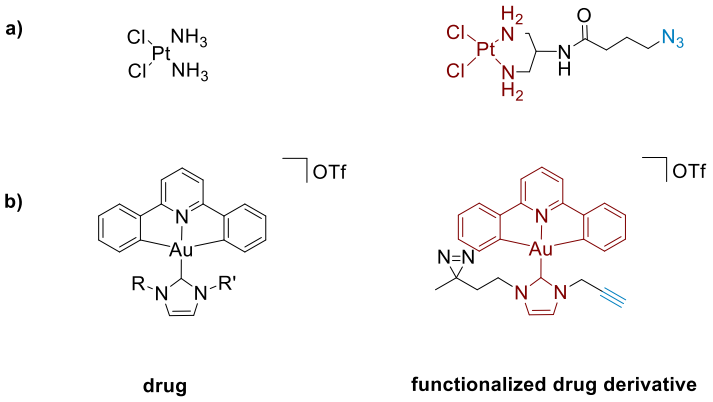

Figure 1.8. Complexes and corresponding probes of drug pull-down experiments of a) the DeRose group and b) the Che group. The enrichment is achieved *via* Cu(I)-catalyzed azide-alkyne cycloaddition.

In addition to pull-down experiments, small click handles also open new opportunities to perform localization experiments in fixed cells. Instead of a label for drug enrichment, a fluorophore moiety can be attached to the complex. This post-treatment labeling allows for the preservation of the biological activity compared to previous methods involving fluorophore-drug derivatives. Introduced by Bierbach and co-workers,[74] the technique was also applied by the groups of DeRose (Scheme 1.5) and Che to localize their drugs in nucleoli and mitochondria of HeLa cells, respectively.[73, 75]

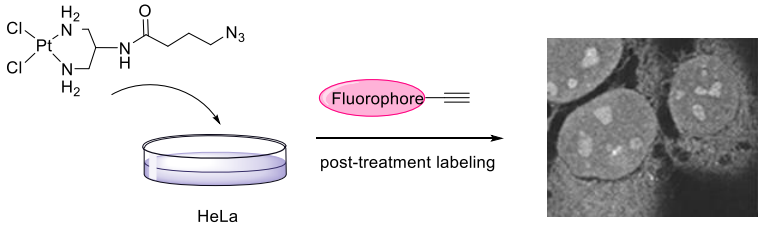

Scheme 1.5. DeRose and co-workers imaged their platinum-based drug in fixed HeLa cells *via* CuAAC after drug treatment. The compound accumulates in the nucleoli of the nucleus.[75]

To conclude, investigations of protein-target interactions and the mode of action of metallodrugs have expanded from controlled reactions with protein models to proteomic studies that revealed the effect of the metallodrug, and even to the analysis of *in vivo* samples. The combination of these approaches allows for a more realistic insight in the fate of the metallodrug in cells. The enrichment of metal-bound proteins by affinity purification or click chemistry allows for the detection of even low abundant binding partners in complex biological samples by MS.

However, so far this approach was associated with rather drastic modifications of the metallodrug (Figure 1.7), which might influence its mode of action and localization.

1.5 Click chemistry for studying metal-protein interactions

1.5.1 Click chemistry as bioorthogonal reaction

The term "click chemistry" was introduced by Sharpless *et al.* in 2001 to describe reactions of a set of modular small building blocks for the easy, reliable, and fast production of larger desired compounds.[76] The reactions need to fulfill the following criteria: "*modular, wide in scope, give very high yields, generate only inoffensive byproducts that can be removed by nonchromatographic methods, and be stereospecific […], simple reaction conditions (ideally, the process should be insensitive to oxygen and water), readily available starting materials and reagents, the use of no solvent or a solvent that is benign (such as water) or easily removed, and simple product isolation*.".[76] Typical examples of such reactions are nucleophilic substitution reactions such as the ring opening of strained heterocyclic electrophiles like epoxides or aziridines, and cycloaddition reactions such as the Diels-Alder reaction and the 1,3-dipolar cycloaddition. The latter is the reaction of two unsaturated molecules to give a five-membered heterocycle, *e.g.* the reaction of an azide and an alkyne resulting in the formation of a triazole (Huisgen 1,3-dipolar cycloaddition, Scheme 1.6a). The non-catalyzed Huisgen 1,3-dipolar cycloaddition requires high temperatures, proceeds with moderate speed and yields a mixture of regioisomers. In 2002, the groups of Sharpless and Meldal independently reported on an improved Huisgen 1,3-dipolar cycloaddition, the copper-catalyzed azide-alkyne cycloaddition (CuAAC, Scheme 1.6b).[77, 78] Depending on the amount of catalytic Cu(I), reaction rates between 10 – 200 $M^{-1} \cdot s^{-1}$ can be achieved for the reaction between an azide and a terminal alkyne.[79] The CuAAC is a biorthogonal reaction: the reagents are not abundant in biological systems and react selectively, their small size minimizes the possibility of perturbations with other biological structures, and the reaction conditions are essentially biocompatible. However, Cu(I) is toxic to cells, which limits the application of this reaction in living systems. To overcome this drawback, Bertozzi *et al.* introduced the strain-promoted [3+2] azide-alkyne cycloaddition (SPAAC, Scheme 1.6c) utilizing cyclooctynes.[80] This reaction is faster than the Huisgen 1,3-dipolar cycloaddition (10^{-2} – 1 $M^{-1} \cdot s^{-1}$), and efficient protein labeling in living systems is reported.[79, 81] However, background fluorescence can occur due to reactions of cyclooctynes with cellular nucleophiles such as glutathione.[82]

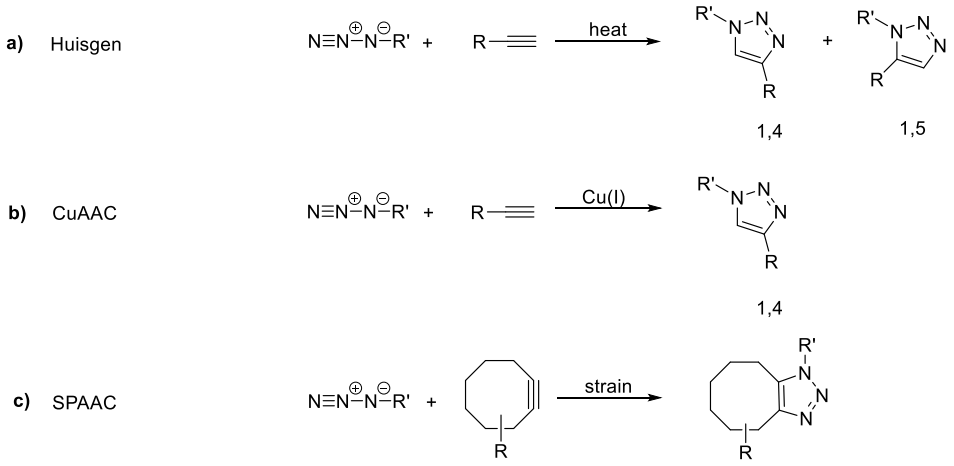

Scheme 1.6. Overview of azide-alkyne reactions.

1.5.2 The CuAAC reaction

The CuAAC can be applied to a wide range of substituted azides and alkynes in high yield (82-94%).[77] The usage of the Cu(I) catalyst leads to an improved regioselectivity since only the 1,4 isomer is formed, to mild reaction conditions (reaction proceeds at room temperature), and to an enhanced reaction rate.[83] Different Cu(I) sources can be used, but the best results are usually obtained when preparing the catalyst *in situ* from Cu(II) salts (like $CuSO_4$) and sodium ascorbate as reductant. The CuAAC reaction can be performed in almost every solvent: non-coordinating, weakly coordinating, polar solvents, as well as in aqueous solutions.[84] The reaction mechanism of the CuAAC is still discussed, and in particular the involvement of one or two Cu(I) centers in catalysis is debated.[85-87] Ligands such as TBTA (tris(benzyltriazolylmethyl)amine), BTTES (bis(tert-butyltriazolmethyl)amine-triazolethyl hydrogen sulfate), THPTA (tris(3-hydroxypropyltriazolylmethyl)amine), have been reported to further decrease the reaction time (Figure 1.9).[88] Those polydentate nitrogen donors bind Cu(I), and stabilize its +1 oxidation state. Therefore, less Cu(I) is required and thus, the reaction is less toxic to cells.[88, 89] Due to the tolerant reaction conditions (wide range of functional groups, solvents, and Cu(I) sources), the CuAAC is used for many applications. It is used in organic synthesis, pharmaceutical science, polymer chemistry, in the synthesis of dendrimers, in material science for surface functionalization,[84, 90] as well as in bioconjugation (like activity-based protein profiling (ABPP) and pull-down assays), as has been summarized in many reviews.[79, 83, 91-93]

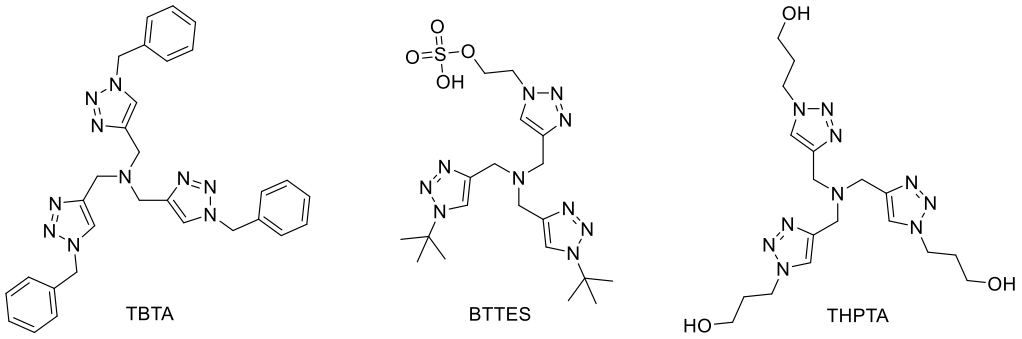

Figure 1.9. Tris(triazolylmethyl)amine ligands for CuAAC applications.

1.6 Aim and outline of this thesis

The goal of the research described in this thesis was to develop a method to functionalize ruthenium polypyridyl complexes suitable for PACT with an alkyne handle. This handle can be utilized in CuAAC to study the localization and mode of action of the PACT compound within cancer cells. Alkyne functionalization is the smallest handle modification possible, and we investigated whether this minimal modification influences the chemical and biological properties of the (pro)drug. The handle enables CuAAC on the complex, and therefore, the labeling of the complex with a reporter tag. The presence of Cu(I) prevents the application in living cells, however, the efficient labeling *via* CuAAC of the ruthenium-based compound would enable localization of the drug in fixed cells with low background fluorescence.

In Chapter 2, the challenging synthesis of an alkyne-functionalized ruthenium polypyridyl complex is described. In addition, fluorophore labeling of the complex *via* CuAAC click chemistry demonstrated that the ruthenium complex interacts with the model protein BSA after light activation. Furthermore, the results showed that fluorescence labeling is a promising method to identify weak non-covalent metal-protein interactions in gel.

In Chapter 3, two new ruthenium-based phototoxic complexes with lipophilic bidentate ligands are introduced. Their light activation, cellular uptake, and singlet oxygen quantum yield were determined and compared to that of [Ru(tpy)(bpy)(Hmte)]$(PF_6)_2$. Depending on the bidentate ligand, the photosubstitution quantum yield can be tuned. In addition, it is shown that the two new complexes are more cytotoxic than their bipyridine analogue due to their

improved cellular uptake. Low singlet oxygen production and light activation in cancer cells supports the true PACT character of these compounds.

In Chapter 4, alkyne-functionalized analogues of the PACT agents introduced in Chapter 3 are reported. Their chemical and biological properties were compared. CuAAC in fixed lung cancer cells allowed for the labeling of the non-emissive ruthenium complexes with a fluorophore. The subcellular location of the labeled complexes was analyzed *via* confocal microscopy imaging and revealed a different mode of action compared to cisplatin.

In Chapter 5, the alkyne functionalization introduced in Chapter 2 was expanded to other polypyridyl ligands coordinated to ruthenium. The known syntheses of the non-functionalized complexes were adjusted to obtain the alkyne analogue complexes. The wide application range of the alkyne functionalization as well as the limitations of this synthesis method are described.

Finally, in Chapter 6, a summary is presented of the main findings described in this thesis, followed by a discussion, and suggestions for further research in this field.

1.7 References

1 B. Rosenberg, L. Van Camp, and T. Krigas, *Nature* **1965**, 205 (4972), 698-699.

2 G. Ciarimboli, *Scientifica* **2012**, 2012 (-), 1-18.

3 J. Reedijk, *Platin. Met. Rev.* **2008**, 52 (1), 2-11.

4 L. Kelland, *Nat. Rev. Cancer* **2007**, 7 (8), 573-584.

5 A. C. Komor and J. K. Barton, *Chem. Commun.* **2013**, 49 (35), 3617-3630.

6 W. Han Ang and P. J. Dyson, *Eur. J. Inorg. Chem.* **2006**, 2006 (20), 4003-4018.

7 A. Bergamo, A. Masi, A. F. A. Peacock, A. Habtemariam, P. J. Sadler, and G. Sava, *J. Inorg. Biochem.* **2010**, 104 (1), 79-86.

8 R. E. Aird, J. Cummings, A. A. Ritchie, M. Muir, R. E. Morris, H. Chen, P. J. Sadler, and D. I. Jodrell, *Br. J. Cancer* **2002**, 86 (10), 1652-1657.

9 H.-K. Liu, S. J. Berners-Price, F. Wang, J. A. Parkinson, J. Xu, J. Bella, and P. J. Sadler, *Angew. Chem.* **2006**, 118 (48), 8333-8336.

10 H. Chen, J. A. Parkinson, R. E. Morris, and P. J. Sadler, *J. Am. Chem. Soc.* **2003**, 125 (1), 173-186.

11 F. Wang, J. Bella, J. A. Parkinson, and P. J. Sadler, *J. Biol. Inorg. Chem.* **2005**, 10 (2), 147-155.

12 R. L. Hayward, Q. C. Schornagel, R. Tente, J. S. Macpherson, R. E. Aird, S. Guichard, A. Habtemariam, P. Sadler, and D. I. Jodrell, *Cancer Chemother Pharmacol* **2005**, 55 (6), 577-583.

13 C. G. Hartinger, S. Zorbas-Seifried, M. A. Jakupec, B. Kynast, H. Zorbas, and B. K. Keppler, *J. Inorg. Biochem.* **2006**, 100 (5), 891-904.

14 C. G. Hartinger, M. A. Jakupec, S. Zorbas-Seifried, M. Groessl, A. Egger, W. Berger, H. Zorbas, P. J. Dyson, and B. K. Keppler, *Chem. Biodiversity* **2008**, 5 (10), 2140-2155.

15 O. Dömötör, C. G. Hartinger, A. K. Bytzek, T. Kiss, B. K. Keppler, and E. A. Enyedy, *J. Biol. Inorg. Chem.* **2013**, 18 (1), 9-17.

16 R. Trondl, P. Heffeter, C. R. Kowol, M. A. Jakupec, W. Berger, and B. K. Keppler, *Chem. Sci.* **2014**, 5 (8), 2925-2932.
17 C. Scolaro, A. Bergamo, L. Brescacin, R. Delfino, M. Cocchietto, G. Laurenczy, T. J. Geldbach, G. Sava, and P. J. Dyson, *J. Med. Chem.* **2005**, 48 (12), 4161-4171.
18 M. Groessl, C. G. Hartinger, P. J. Dyson, and B. K. Keppler, *J. Inorg. Biochem.* **2008**, 102 (5–6), 1060-1065.
19 B. Wu, M. S. Ong, M. Groessl, Z. Adhireksan, C. G. Hartinger, P. J. Dyson, and C. A. Davey, *Chem. Eur. J.* **2011**, 17 (13), 3562-3566.
20 A. Casini, C. Gabbiani, E. Michelucci, G. Pieraccini, G. Moneti, P. Dyson, and L. Messori, *J. Biol. Inorg. Chem.* **2009**, 14 (5), 761-770.
21 A. Casini, C. Gabbiani, F. Sorrentino, M. P. Rigobello, A. Bindoli, T. J. Geldbach, A. Marrone, N. Re, C. G. Hartinger, P. J. Dyson, and L. Messori, *J. Med. Chem.* **2008**, 51 (21), 6773-6781.
22 A. R. Timerbaev, C. G. Hartinger, S. S. Aleksenko, and B. K. Keppler, *Chem. Rev.* **2006**, 106 (6), 2224-2248.
23 A. V. Rudnev, S. S. Aleksenko, O. Semenova, C. G. Hartinger, A. R. Timerbaev, and B. K. Keppler, *J. Sep. Sci.* **2005**, 28 (2), 121-127.
24 A. Casini and J. Reedijk, *Chem. Sci.* **2012**, 3 (11), 3135-3144.
25 M. P. Sullivan, H. U. Holtkamp, and C. G. Hartinger, Antitumor Metallodrugs that Target Proteins in *Metallo-Drugs: Development and Action of Anticancer Agents* **2018**, 351-386.
26 E. Meggers, *Chem. Commun.* **2009**, - (9), 1001-1010.
27 G. Sava, G. Jaouen, E. A. Hillard, and A. Bergamo, *Dalton Trans.* **2012**, 41 (27), 8226-8234.
28 A. K. Renfrew, A. D. Phillips, E. Tapavicza, R. Scopelliti, U. Rothlisberger, and P. J. Dyson, *Organometallics* **2009**, 28 (17), 5061-5071.
29 N. Graf and S. J. Lippard, *Adv. Drug Delivery Rev.* **2012**, 64 (11), 993-1004.
30 U. Jungwirth, C. R. Kowol, B. K. Keppler, C. G. Hartinger, W. Berger, and P. Heffeter, *Antioxid. Redox Signaling* **2011**, 15 (4), 1085-1127.
31 M. D. Daniell and J. S. Hill, *ANZ J Surg* **1991**, 61 (5), 340-348.
32 D. E. J. G. J. Dolmans, D. Fukumura, and R. K. Jain, *Nat. Rev. Cancer* **2003**, 3 (-), 380-387.
33 G. Shi, S. Monro, R. Hennigar, J. Colpitts, J. Fong, K. Kasimova, H. Yin, R. DeCoste, C. Spencer, L. Chamberlain, A. Mandel, L. Lilge, and S. A. McFarland, *Coord. Chem. Rev.* **2015**, 282-283 127-138.
34 Y. Arenas, S. Monro, G. Shi, A. Mandel, S. McFarland, and L. Lilge, *Photodiagnosis Photodyn. Ther.* **2013**, 10 (4), 615-625.
35 P. Agostinis, K. Berg, K. A. Cengel, T. H. Foster, A. W. Girotti, S. O. Gollnick, S. M. Hahn, M. R. Hamblin, A. Juzeniene, D. Kessel, M. Korbelik, J. Moan, P. Mroz, D. Nowis, J. Piette, B. C. Wilson, and J. Golab, *CA: Cancer J. Clin.* **2011**, 61 (4), 250-281.
36 B. Muz, P. de la Puente, F. Azab, and A. K. Azab, *Hypoxia (Auckland, N.Z.)* **2015**, 3 (-), 83-92.
37 P. Stadler, A. Becker, H. Jürgen Feldmann, G. Hänsgen, J. Dunst, F. Würschmidt, and M. Molls, *Int. J. Radiat. Oncol., Biol., Phys.* **1999**, 44 (4), 749-754.
38 N. J. Farrer, L. Salassa, and P. J. Sadler, *Dalton Trans.* **2009**, - (48), 10690-10701.
39 S. Bonnet, *Dalton Trans.* **2018**, 47 (31), 10330-10343.
40 V. H. S. van Rixel, B. Siewert, S. L. Hopkins, S. H. C. Askes, A. Busemann, M. A. Siegler, and S. Bonnet, *Chem. Sci.* **2016**, 7 (8), 4922-4929.
41 L. N. Lameijer, T. G. Brevé, V. H. S. van Rixel, S. H. C. Askes, M. A. Siegler, and S. Bonnet, *Chem. Eur. J.* **2018**, 24 (11), 2709-2717.
42 A. Li, C. Turro, and J. J. Kodanko, *Chem. Commun.* **2018**, 54 (11), 1280-1290.

43 M. Huisman, J. K. White, V. G. Lewalski, I. Podgorski, C. Turro, and J. J. Kodanko, *Chem. Commun.* **2016**, 52 (85), 12590-12593.

44 T. N. Rohrabaugh, A. M. Rohrabaugh, J. J. Kodanko, J. K. White, and C. Turro, *Chem. Commun.* **2018**, 54 (41), 5193-5196.

45 J.-A. Cuello-Garibo, M. S. Meijer, and S. Bonnet, *Chem. Commun.* **2017**, 53 (50), 6768-6771.

46 L. N. Lameijer, D. Ernst, S. L. Hopkins, M. S. Meijer, S. H. Askes, S. E. Le Dévédec, and S. Bonnet, *Angew. Chem., Int. Ed.* **2017**, 56 (38), 11549-11553.

47 J.-A. Cuello-Garibo, C. C. James, M. A. Siegler, and S. Bonnet, *Chem. Sq* **2017**, 1 (2), 1-19.

48 A. Bijelic, S. Theiner, B. K. Keppler, and A. Rompel, *J. Med. Chem.* **2016**, 59 (12), 5894-5903.

49 A. Casini, A. Guerri, C. Gabbiani, and L. Messori, *J. Inorg. Biochem.* **2008**, 102 (5), 995-1006.

50 L. Trynda-Lemiesz, A. Karaczyn, B. K. Keppler, and H. Kozlowski, *J. Inorg. Biochem.* **2000**, 78 (4), 341-346.

51 M. Groessl and P. J. Dyson, *Curr. Top. Med. Chem.* **2011**, 11 (21), 2632-2646.

52 A. Casini, G. Mastrobuoni, W. H. Ang, C. Gabbiani, G. Pieraccini, G. Moneti, P. J. Dyson, and L. Messori, *ChemMedChem* **2007**, 2 (5), 631-635.

53 A. Casini, A. Karotki, C. Gabbiani, F. Rugi, M. Vasak, L. Messori, and P. J. Dyson, *Metallomics* **2009**, 1 (5), 434-441.

54 C. G. Hartinger, A. Casini, C. Duhot, Y. O. Tsybin, L. Messori, and P. J. Dyson, *J. Inorg. Biochem.* **2008**, 102 (12), 2136-2141.

55 M. Groessl, O. Zava, and P. J. Dyson, *Metallomics* **2011**, 3 (6), 591-599.

56 M.-Y. Ho, M.-L. Chiou, R.-C. Chang, Y.-H. Chen, and C.-C. Cheng, *J. Inorg. Biochem.* **2010**, 104 (5), 614-617.

57 C. G. Hartinger, M. Groessl, S. M. Meier, A. Casini, and P. J. Dyson, *Chem. Soc. Rev.* **2013**, 42 (14), 6186-6199.

58 H. U. Holtkamp and C. G. Hartinger, *Trends Anal. Chem.* **2018**, 104 (-), 110-117.

59 C. Artner, H. U. Holtkamp, W. Kandioller, C. G. Hartinger, S. M. Meier-Menches, and B. K. Keppler, *Chem. Commun.* **2017**, 53 (57), 8002-8005.

60 I. Khalaila, A. Bergamo, F. Bussy, G. Sava, and P. J. Dyson, *Int. J. Oncol.* **2006**, 29 (1), 261-268.

61 M.-Y. Ho, M.-L. Chiou, W.-S. Du, F. Y. Chang, Y.-H. Chen, Y.-J. Weng, and C.-C. Cheng, *J. Inorg. Biochem.* **2011**, 105 (6), 902-910.

62 M. P. Washburn, D. Wolters, and J. R. Yates, *Nat Biotech* **2001**, 19 (3), 242-247.

63 J. Will, A. Kyas, W. Sheldrick, and D. Wolters, *J. Biol. Inorg. Chem.* **2007**, 12 (6), 883-894.

64 R. F. S. Lee, A. Chernobrovkin, D. Rutishauser, C. S. Allardyce, D. Hacker, K. Johnsson, R. A. Zubarev, and P. J. Dyson, *Scientific Reports* **2017**, 7 (1), 1590-1600.

65 S. P. Gygi, B. Rist, S. A. Gerber, F. Turecek, M. H. Gelb, and R. Aebersold, *Nat. Biotech.* **1999**, 17 (10), 994-999.

66 T. W. Hutchens and T.-T. Yip, *Rapid Commun. Mass Spectrom.* **1993**, 7 (7), 576-580.

67 M. V. Babak, S. M. Meier, K. V. M. Huber, J. Reynisson, A. A. Legin, M. A. Jakupec, A. Roller, A. Stukalov, M. Gridling, K. L. Bennett, J. Colinge, W. Berger, P. J. Dyson, G. Superti-Furga, B. K. Keppler, and C. G. Hartinger, *Chem. Sci.* **2015**, 6 (4), 2449-2456.

68 S. M. Meier, D. Kreutz, L. Winter, M. H. M. Klose, K. Cseh, T. Weiss, A. Bileck, B. Alte, J. C. Mader, S. Jana, A. Chatterjee, A. Bhattacharyya, M. Hejl, M. A. Jakupec, P. Heffeter, W. Berger, C. G. Hartinger, B. K. Keppler, G. Wiche, and C. Gerner, *Angew. Chem., Int. Ed.* **2017**, 56 (28), 8267-8271.

69 J. D. White, M. F. Osborn, A. D. Moghaddam, L. E. Guzman, M. M. Haley, and V. J. DeRose, *J. Am. Chem. Soc.* **2013**, 135 (32), 11680-11683.

70 M. F. Osborn, J. D. White, M. M. Haley, and V. J. DeRose, *ACS Chem. Biol.* **2014**, 9 (10), 2404-2411.
71 R. M. Cunningham and V. J. DeRose, *ACS Chem. Biol*. **2017**, 12 (11), 2737-2745.
72 D. Hu, Y. Liu, Y.-T. Lai, K.-C. Tong, Y.-M. Fung, C.-N. Lok, and C.-M. Che, *Angew. Chem., Int. Ed.* **2016**, 55 (4), 1387-1391.
73 S. K. Fung, T. Zou, B. Cao, P.-Y. Lee, Y. M. E. Fung, D. Hu, C.-N. Lok, and C.-M. Che, *Angew. Chem.* **2017**, 129 (14), 3950-3954.
74 S. Ding, X. Qiao, J. Suryadi, G. S. Marrs, G. L. Kucera, and U. Bierbach, *Angew. Chem.* **2013**, 125 (12), 3434-3438.
75 R. Wirth, J. D. White, A. D. Moghaddam, A. L. Ginzburg, L. N. Zakharov, M. M. Haley, and V. J. DeRose, *J. Am. Chem. Soc.* **2015**, 137 (48), 15169-15175.
76 H. C. Kolb, M. G. Finn, and K. B. Sharpless, *Angew. Chem., Int. Ed.* **2001**, 40 (11), 2004-2021.
77 V. V. Rostovtsev, L. G. Green, V. V. Fokin, and K. B. Sharpless, *Angew. Chem., Int. Ed.* **2002**, 41 (14), 2596-2599.
78 C. W. Tornøe, C. Christensen, and M. Meldal, *J. Org. Chem.* **2002**, 67 (9), 3057-3064.
79 K. Lang and J. W. Chin, *ACS Chem. Biol.* **2014**, 9 (1), 16-20.
80 N. J. Agard, J. A. Prescher, and C. R. Bertozzi, *J. Am. Chem. Soc.* **2004**, 126 (46), 15046-15047.
81 N. J. Agard, J. M. Baskin, J. A. Prescher, A. Lo, and C. R. Bertozzi, *ACS Chem. Biol.* **2006**, 1 (10), 644-648.
82 C. S. McKay and M. G. Finn, *Chem. Biol.* **2014**, 21 (9), 1075-1101.
83 M. D. Best, *Biochemistry* **2009**, 48 (28), 6571-6584.
84 L. Liang and D. Astruc, *Coord. Chem. Rev.* **2011**, 255 (23), 2933-2945.
85 V. O. Rodionov, V. V. Fokin, and M. G. Finn, *Angew. Chem.* **2005**, 117 (15), 2250-2255.
86 M. Meldal and C. W. Tornøe, *Chem. Rev.* **2008**, 108 (8), 2952-3015.
87 B. T. Worrell, J. A. Malik, and V. V. Fokin, *Science* **2013**, 340 (6131), 457-460.
88 C. Besanceney-Webler, H. Jiang, T. Zheng, L. Feng, D. Soriano del Amo, W. Wang, L. M. Klivansky, F. L. Marlow, Y. Liu, and P. Wu, *Angew. Chem., Int. Ed.* **2011**, 50 (35), 8051-8056.
89 V. Hong, N. F. Steinmetz, M. Manchester, and M. G. Finn, *Bioconjugate Chem.* **2010**, 21 (10), 1912-1916.
90 C. D. Hein, X.-M. Liu, and D. Wang, *Pharm. Res.* **2008**, 25 (10), 2216-2230.
91 C. P. Ramil and Q. Lin, *Chem. Commun.* **2013**, 49 (94), 11007-11022.
92 D. M. Patterson, L. A. Nazarova, and J. A. Prescher, *ACS Chem. Biol.* **2014**, 9 (3), 592-605.
93 E. M. Sletten and C. R. Bertozzi, *Angew. Chem., Int. Ed.* **2009**, 48 (38), 6974-6998.